Etching and printing of diffractive optical microstructures by a femtosecond excimer laser

Etching and printing of diffractive optical microstructures by a femtosecond excimer laser

Sakellaris Mailis, Ioanna Zergioti, George Koundourakis, Aris Ikiades,
Argyro Patentalaki, Pagona Papakonstantinou, Nikolaos A. Vainos, and Costas Fotakis

Diffractive optics fabrication is performed by two complementary processing methods that rely on the photoablation of materials by ultrashort UV laser pulses. The spatially selective ablation of materials permits the direct microetching of high-quality surface-relief patterns. In addition, the direct, spatially selective transfer of the ablated material onto planar and nonplanar receiving substrates provides a complementary microprinting operation. The radiation from the ultrashort pulsed excimer laser results in superior quality at relatively low-energy density levels, owing to the short absorption length and minimal thermal-diffusion effects. Computer-generated holographic structures are produced by both modes of operation. Submicrometer features, including Bragg-type structures, are microprinted onto planar and high-curvature optical-fiber surfaces, demonstrating the unique ability of the schemes for complex microstructure and potentially nanostructure development.
OCIS codes: 220.4000, 230.3990, 050.1970, 060.2370, 200.4650.

1. Introduction

Computer-generated holograms (CGH's), diffractive optical elements, and other micro-optics are currently attracting increasing interest in their wider use in optoelectronics.[1] Current research is not only associated with hologram design optimization but also with the development of new fabrication methods aimed at achieving greater simplicity and flexibility and lower fabrication costs. The well-established microfabrication methods combining a number of processing steps such as lithography and reactive ion etching,[2] or ion exchange[3] and thin-film deposition,[4] are inherently complex and expensive. In several cases involving nonplanar, high-curvature segmented-surface or high-strength material's processing, these conventional but well-established schemes have been unable to produce the required results. Furthermore, in the context of micro-electro-mechanics,[5] the introduction of novel optical concepts would certainly lead to further technological advances.

Direct laser-based methods for the fabrication of microstructures provide an alternative, relatively simple, and cost-effective approach. New developments in optoelectronics and micro-electro-mechanics and the prospective mass-production needs justify an increasing effort toward the investigation of such new fabrication methods aimed at versatile, cost-effective, high-quality structure development. On the one hand, high-intensity UV excimer-laser radiation has been utilized to demonstrate the direct etching of surface-relief diffractive microstructures by selective ablation of materials[6] and also later by waveguide excimer lasers with high pulse repetition rates.[7] On the other hand, the potential for obtaining the selective microdeposition of relatively large metallic structures onto a surface has also been demonstrated[8,9] by the direct writing of 50-μm-wide Cu lines with nanosecond excimer and Nd:YAG laser pulses under high vacuum (10^{-6} mbar). The deposition of 100-μm-wide patterns of superconducting thin films with nanosecond ArF excimer and Nd:YAG lasers has also been reported.[10,11]

Both methods may be applied either in a direct

When this research was done, the authors were with the Laser and Applications Division, Institute of Electronic Structure and Laser, Foundation for Research and Technology-Hellas, P.O. Box 1527, Heraklion 71110, Greece. S. Mailis is now with the Optoelectronics Research Centre, University of Southampton, Highfield, Southampton SO17 1BJ, UK. I. Zergioti is now with the Max Planck Institut fur Biophysikalische Chemie, P.O. Box 2841, 37018 Gottingen, Germany. P. Papakonstantinou is now with Northern Ireland Bio-engineering Research Centre, School of Electrical and Mechanical Engineering, University of Ulster, Newtownabbey, Co. Antrim BT37 OQB, Northern Ireland, UK. N. A. Vainos's e-mail address is vainos@iesl.forth.gr

Received 22 June 1998; revised manuscript received 2 November 1998.
0003-6935/99/112301-08$15.00/0

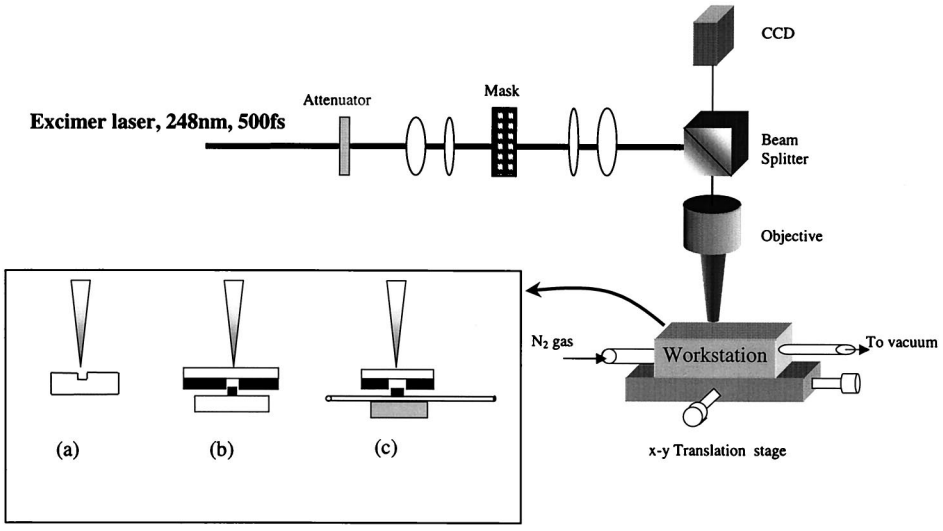

Fig. 1. Experimental layout for direct excimer-laser microfabrication. Inset: (a) microetching, (b) microprinting, (c) microprinting on optical fibers.

mask-projection pattern-transfer mode or in a pixel-by-pixel step-and-repeat operation. In the latter case a slit that is usually rectangular is projected in raster across the surface of the receiving substrate to produce the required pattern.

Laser ablation by nanosecond excimer-laser pulses is seen to exhibit significant thermal effects,[12,13] naturally depending on the physical properties of the target material. Comparative studies[14,15] concerning laser-pulse duration verify that subpicosecond laser radiation may be more suitable for such applications. Ultrashort UV laser pulses minimize thermal effects,[16,17] because absorption and thermal-diffusion lengths are kept to a minimum. In this regime, multiphoton electron ionization and electron-lattice energy coupling dominate, whereas the avalanche breakdown process initiated by single ionized electrons plays a secondary role. Depending always on the thermophysical properties of the materials, the melting zone front is greatly reduced with a corresponding increase in the vaporization zone, even at near-IR laser wavelengths.[18]

The effects outlined above lower the ablation threshold values and further reduce their statistical spread. Geometric spatial-filtering methods have thus produced high-quality etching of even submicrometer regular periodic grating structures.[19] Furthermore the selective microdeposition technique has been advanced further, and very recently submicrometer features have been successfully deposited by ultrashort excimer-laser pulses in low-vacuum conditions.[20]

In this research we extend our discussion on the application of the microablation methods of ultrashort pulsed lasers and demonstrate two reliable single-step microfabrication modes of operation. By relying on purely physical processes, one removes material selectively from the substrate surface, leaving behind a precisely etched surface-relief pattern. In the second and complementary operation the material ablated from a thin-film source is transferred precisely onto the substrate, producing again a surface-relief printed pattern with submicrometer resolution.

Diffractive optics are successfully produced, first, by microetching and, second, by the complementary microprinting operation. The high-definition, high-aspect-ratio, surface-relief patterns produced are the result of very precise noncontact removal of materials and transfer processes. CGH's and Bragg-type microstructures are fabricated onto planar, segmented, and high-curvature surfaces by high-intensity 500-fs UV excimer-laser pulses at a wavelength of 248 nm. The selective microablation process embraces a combination of advantageous features of high-resolution imaging, threshold reduction, and stabilization as well as minimal thermal effects. Furthermore the microprinting method has been used for the first time to our knowledge for fabricating submicrometer structures onto highly curved surfaces of radii of less than 20 μm, addressing here optical-fiber-based systems. This unique operation, particularly relevant to sensor applications, constitutes a major step forward and verifies the versatility and the potential of the methods presented.

2. Experimental Procedures

The experimental configuration is depicted schematically in Fig. 1. The optical system is based on the inverse microscope principle, and it is configured with a hybrid distributed-feedback dye-laser/excimer-laser femtosecond system delivering 500-fs pulses and 5–20 mJ of energy per pulse at 248 nm with a 10-Hz maximum pulse repetition rate. A specially designed laser-beam delivery system is also used, incorporating the spatial modulation of the beam by a chrome-on-quartz mask or a single slit. The demagnification projection ratio is approximately 30:1 and may be conveniently amended. No temporal pulse dispersion is observed. The device is

equipped with a pair of high-precision X–Y piezoelectric translation stages offering a 50-nm translation resolution determined by optical encoders across a 25 mm $\times$ 25 mm area. Both laser and translation stages are computer controlled, and the working area is viewed through the microscope ocular lenses and a CCD camera. By utilizing the raster-scanning fabrication mode, the construction of masks is facilitated by the same system, eliminating therefore the need for complicated lithographic methods. The masks produced are subsequently used for fabricating diffractive structures. Multiperiodic masks can thus be constructed, and the process can be optimized to achieve a cost-effective operation.

In the microetching mode the substrate is placed right under the microscope objective as shown in Fig. 1, inset (a). Selective ablation of the material is performed, achieving surface-relief patterning with high spatial and depth resolution. The substrate is translated on the X–Y plane by the piezoelectric translation stages to form multiperiodic structures in a step-and-repeat fashion. Microetching in the raster mode was mainly applied for the construction of the master CGH masks.

In the microprinting operation a receiver substrate is placed near contact to a fused silica target source by use of an especially developed miniature cell. The miniature cell operates in a partial vacuum at a pressure of 10^{-1} Torr. The transparent target source comprises a thin film of the material to be deposited. In these experiments evaporated Cr thin films as well as pulsed-laser-deposited InO_x thin films were used. The UV laser beam was focused through the fused silica plate onto the thin-film surface as shown in Fig. 1, inset (b). The selectively ablated material is ejected from the source codirectionally to the laser beam and deposited onto the receiving substrate. Selective deposition of the material in this forward-transfer mode is thus performed, establishing a microprinting operation. A variety of receiving optical surfaces including glass, silicon, and zinc selenide have been used. For performing the operation onto optical-fiber surfaces a special attachment has been developed to achieve close contact of the fiber and the planar source [Fig. 1, inset (c)]. The optical fibers have been chemically etched to access the core area, and radii of curvature as small as 18 μm have been used. An even smaller distance to the fiber core would be appropriate to facilitate interaction between the guided wave and the microstructure or to provide evanescent wave coupling. Further research in this direction involving asymmetric etching is in progress.

Single-pixel or single-period master masks were used for the spatial modulation of the UV beam. Relatively large arrays of this single-period pattern could be produced in a consecutive step-and-repeat manner. Typical laser-fluence values for microetching and microprinting were in the range of 30–650 mJ/cm^2. A scanning electron microscope (SEM) and an atomic force microscope (AFM) were applied to assess the quality of the patterns. Stylus profilometry is not applicable in our case owing to the small features involved.

3. Results and Discussion

A. Ultrashort Laser-Pulse Microetching

In the microetching mode the excimer-laser beam directly illuminates the optical surface. For energy fluence above the ablation threshold (a threshold strongly dependent on material properties) material removal occurs with high precision. The short absorption length and the negligible thermal diffusion for ultrashort pulsed radiation result in rapid plasma formation from the solid. The liquid zone is usually of negligible extent, naturally depending on the properties of the materials. Several materials were used in the direct etching mode including a range of polymers, such as poly (methyl methacrylate) (PMMA), polycarbonate, polyimide, photoresist, as well as metals and metal alloys such as copper, aluminum, and stainless steel. In most cases a very limited thermally affected zone is observed, and well-defined, good-aspect-ratio etching results are obtained. Furthermore debris accumulation observed with nanosecond pulses is also seen to be limited. Etching quality deteriorates only at high fluence levels (>1 J/cm^2) and very deep (several microns) etching, both of which are inappropriate for the present application.

Preliminary studies of the etching characteristics were carried out for determining threshold ED_{th} (mJ/cm^2) and etching rate (nanometer per pulse) values for the materials used. Such a procedure is of extreme importance here because it defines the range of operational parameters for achieving high-quality etching and consequently the appropriate phase steps for the diffractive structures. Although the aim of the present research is not to provide a detailed comparison between nanosecond and subpicosecond operation, the dependence of the etching rates on the laser fluence has been investigated comparatively to highlight differences and provide guidance for subsequent experiments.

Denotative etching results obtained here for PMMA, polycarbonate, aluminum, and stainless steel are plotted in Fig. 2. Data from using 20-ns pulses at 248 nm and exactly the same experimental configuration are included for comparison. In all cases a well-stabilized, almost linear etch rate (nm pulse^{-1}) is observed. Note the steeper slopes and the absence of saturation for the fluence levels reached. A dramatic decrease in the single-pulse etching-threshold value that is also observed in most cases must be underlined. This value represents the fluence level at the target required for ablative removal of material to be induced from a perfectly new target in a single-pulse experiment. In contrast the etching-threshold values obtained in multipulse experiments are naturally lower, because gradual radiation deterioration of the material's surface enhances the ablation process. Such effects are responsible for the apparent higher etching rates ob-

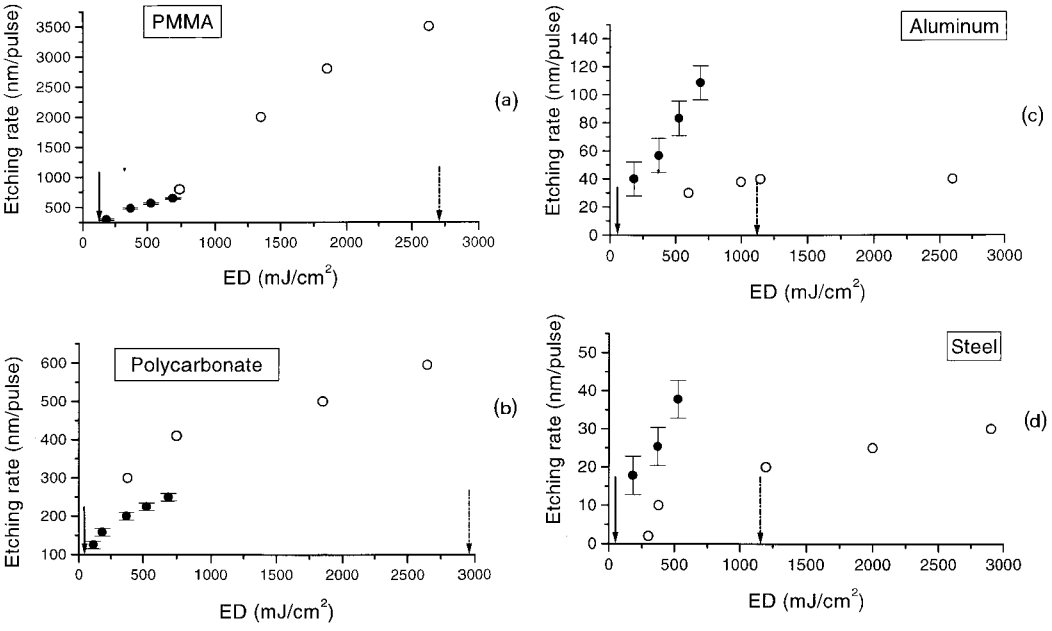

Fig. 2. Etching rate versus excimer-laser fluence, ED, for (a), PMMA; (b), polycarbonate; (c), aluminum; (d), stainless steel, for 500-fs (solid circles) and 20-ns (open circles) laser pulses at 248 nm. Arrows indicate the single-pulse threshold fluence: solid arrow, 500-fs pulses; dot–dash arrow, 20-ns pulses.

served in polymers for nanosecond pulses with, however, a dramatic decrease in etching quality.

It has been proved, generally, difficult to achieve in practice the optimum etch depth for a π-phase shift by looking up a predefined table. This difficulty is mainly due to the instability of the energy level and the profile of the laser beam. For a reliable performance an on-line system for monitoring diffraction efficiency[6] can be incorporated for optimum operation. Nevertheless the most emphasis here is to the production of high-quality clean etching without applying additional processing or laser-beam shaping. Therefore the energy density on the target was kept relatively high to alleviate such laser-output instabilities. Optimization procedures are not included in this research and represent a further step.

The computer-generated holographic structures presented have been fabricated here mainly by direct projection and replication of a single-period master mask. Multiperiodic structures were etched for maximum diffraction efficiency and holographic fidelity. This arrangement was found to be convenient for reducing respective fabrication time and costs, since a large part of the pattern is transferred to the optical surface in a single step. As we have emphasized above, the pixelated (raster) mode has been applied only to the construction of masks.

A SEM picture of a fanout CGH etched on PMMA is depicted in Fig. 3(a). This pattern of 4×4 replications of the master hologram period was fabricated in a step-and-repeat manner. In this example the minimum feature lateral size (pixel) of the etched pattern is $\lesssim 2$ μm. The etching-laser energy density was 395 mJ/cm^2, and six pulses were arbitrarily used to provide a second phase level. In Fig. 3(b) an AFM image of part of the hologram is shown. The rectangular pixel geometry is apparent, and the measured rms etch roughness is $\sim$200 nm. The etch aspect ratio is in the range of 3:1–5:1, depending on the hologram area. The etch depth estimated by SEM image-projection methods is $\sim 2.1 \pm 0.2$ μm and corresponds to a phase step of $\sim 3.26\pi$ for 633-nm radiation. Detailed AFM analysis reveals a 2.3-μm average depth with a 10% uniformity over a 60 μm $\times$ 60 μm area. This analysis represents an average phase step of $\sim 3.5\pi$. Although this improper phase step is produced, an acceptable hologram reconstruction of the etched CGH is obtained as shown in Fig. 3(c). The measured diffraction efficiency is relatively low at $\sim$10% (uncorrected for Fresnel and scattering losses) but is in line with rigorous coupled-wave analysis results indicating a maximum theoretical value of $\sim$20%. The reconstructed beamlet uniformity [defined as $\{1 - \sigma(I)/\langle I \rangle\}$] is $\sim$75%. Note that for a large-area etching the spatial laser-beam inhomogeneity is an additional factor enhancing surface roughness. No beam homogenization or surface posttreatment has been applied here.

Other types of specialized optics have also been fabricated including Fresnel-type fanout CGH elements and holograms in alloys of high mechanical strength such as steel. In addition generic CGH patterns have been produced. The example in Fig. 4(a) is a Fourier CGH etched on polyimide. Hologram reconstruction by a HeNe laser beam produces the alphanumeric sentence THIS IS NOT A HOLOGRAM 0123456789 in Fig. 4(b). Such an operation may be useful in holographic security applications. Holograms can be directly (or indirectly by replication) produced on the surface of the item of interest, whereas subsequent readout provides the required

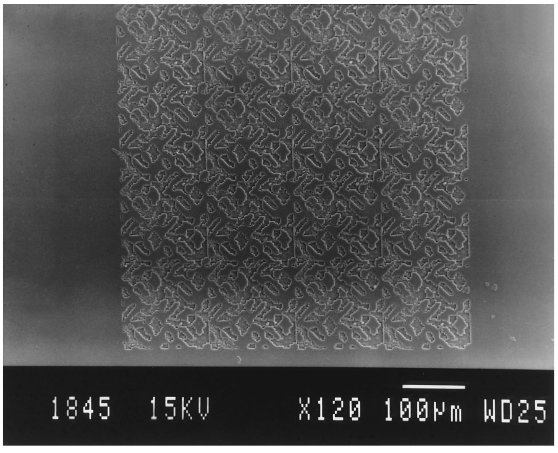

(a)

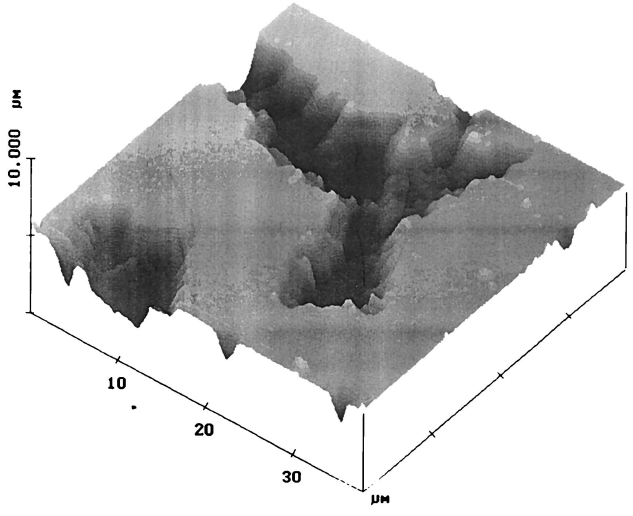

(b)

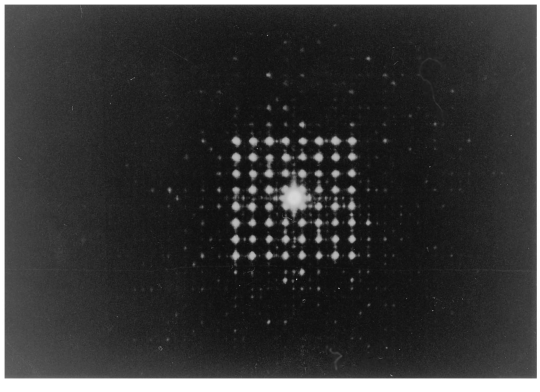

(c)

Fig. 3. Fanout element etched in PMMA: (a) SEM picture, (b) AFM image, (c) hologram reconstruction at 633 nm.

pass operation. Further optical encryption may also be applied.

As a general comment, radiation from the femtosecond pulsed laser facilitates the production of microetching of higher quality than in the case of nanosecond pulses at the same wavelength of 248 nm.[6] Features are well defined, owing to the short absorption length (additionally enhanced by means of nonlinear processes) and minimal thermal diffusion, which results in a cleaner cut of the material's surface. The well-defined microetched features are formed with crater walls exhibiting a greater aspect ratio. Short absorption lengths may be well met even when near-IR femtosecond pulses (produced, for example, by a Ti:sapphire laser) are used, owing to the multiphoton absorption processes involved. In this latter case, however, the imaging resolution is inferior, owing to the 3× longer wavelength and the higher degree of coherence attained. In addition, some thermal effects would be apparent in that case, caused by the greater penetration of the relatively low-intensity wings of the laser beam/pattern. Because the processes involved are heavily dependent on the material's nature, the particular application sought defines the range of the operational parameters.

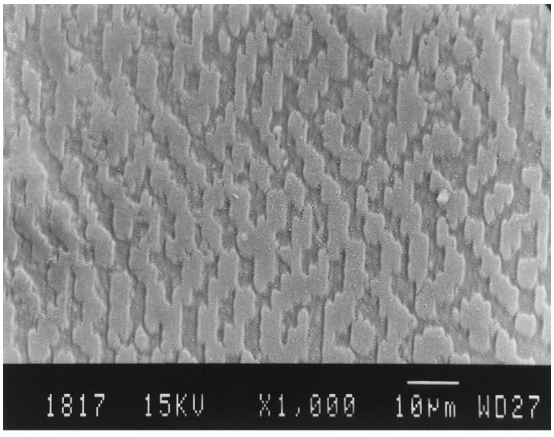

(a)

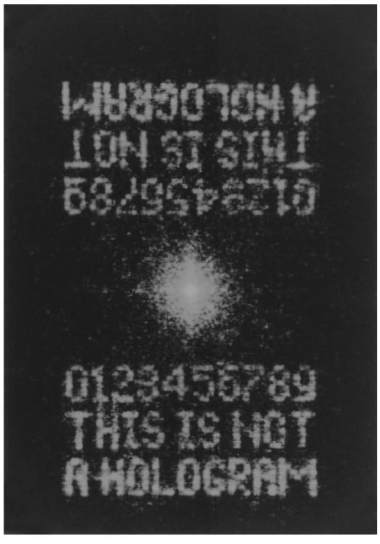

(b)

Fig. 4. (a) Generic-pattern CGH structure etched on polyimide and (b) CGH reconstruction of an alphanumeric sentence at 633 nm.

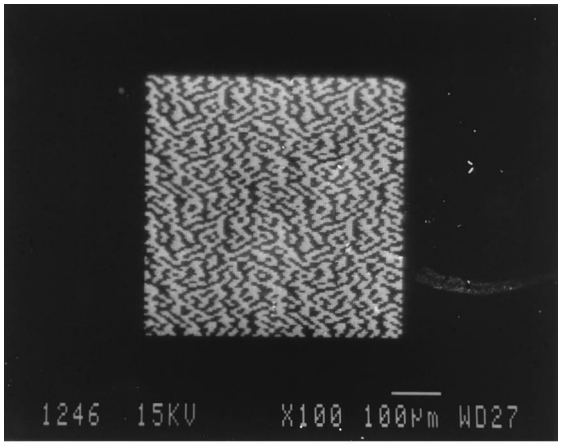

(a)

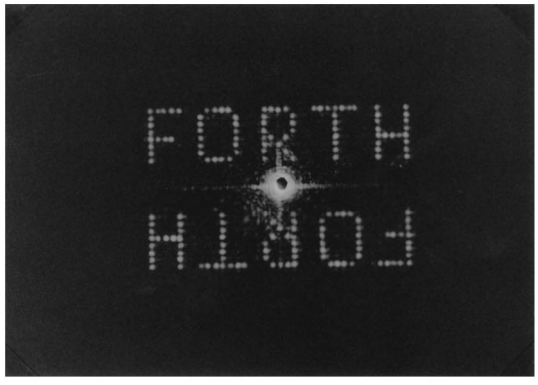

(b)

Fig. 5. (a) Raster microprinted Cr on a glass CGH pattern and (b) CGH reconstruction at 633 nm.

B. Microprinting onto Planar Surfaces

In the microprinting operation the target material is deposited on fused silica substrates and placed near contact to the receiving optical surface. The mask illuminated by the femtosecond excimer laser is projected demagnified onto the surface of the thin film through the supporting substrate. The illuminated part of the thin film is selectively ablated in the forward direction and deposited onto the optical surface, as shown in Fig. 1, insets (b) and (c). The microstructures deposited exhibit exceptional adherence in most cases.

Two types of source films have been used in the present experiments. Sputtered Cr films of 400–800 Å exhibit an absorption depth of ~75 Å. InO_x films of 450–2200-Å thickness have been prepared by reactive pulsed excimer-laser deposition in oxygen atmosphere[21] and exhibited an absorption depth of ~400 Å. It is clear that in both cases most of the energy is absorbed near the substrate–film interface. Thermal diffusion is negligible compared with the time scale of the pulse duration, ensuring a rapid expansion of the ablated front from this interface. We note here that nonlinear absorption further reduces penetration depth. The complex nature of this process is currently under investigation.[20]

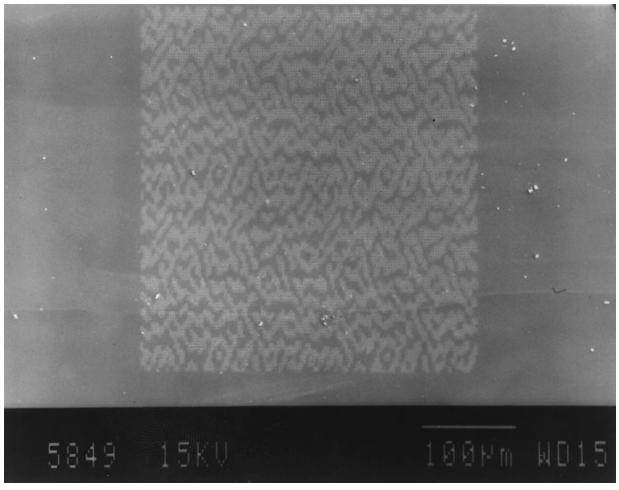

Fig. 6. Computer-generated holographic pattern of amorphous/polycrystalline InO_x on glass.

However, depending on the projected spot energy profile, only a limited area may be above threshold and therefore becomes ablated. In effect the ejected material can be of limited extent, producing submicrometer-size deposited features in a quite reproducible fashion.

A SEM photograph of a microdeposited CGH structure of Cr deposited on glass is shown in Fig. 5(a). This diffractive structure is deposited pixel by pixel with a pixel size of 4 μm × 4 μm. Upon illumination by HeNe laser radiation, FORTH is reproduced as shown in Fig. 5(b). This CGH is a purely absorptive element, which, however, operates well with the exception of the expected strong zero-order (dc) scattering component. Owing to loss, the diffraction efficiency is relatively low with typical values measured here in the range of 5%.

Microprinting diffractive structures by single-period master-mask projection is also demonstrated. This operation is cost-effective because a large part of the pattern is produced in a single laser shot. Step-and-repeat operation is also performed, and the adherence of features is also excellent. Various optical surfaces including silicon and zinc–selenide substrates have also been used with good results.

Indium oxide (InO_x) exhibits interesting electrical and optical properties including the demonstration of holographic recording in amorphous and polycrystalline material.[21] Indium oxide patterns were grown in a forward-transfer mode by use of film sources of 45–220-nm thickness, as discussed above. Figure 6 depicts a CGH pattern produced by microprinting from a 200-nm-thick polycrystalline InO_x target source on glass at an energy density of 150 mJ/cm^2 with a pixel size of 4 μm × 4 μm. In other experiments the production of microdots having the same crystalline properties as the source material has been achieved. The potential for obtaining submicrometer-size optically active elements will be discussed elsewhere.

C. Microstructures on Optical Fibers

Microprinting micrometer and submicrometer structures onto nonplanar surfaces, including segmented, discontinuous, or high-curvature surfaces, provides a unique means for developing miniature passive and potentially active structures. In this research we have addressed this operation in the context of optical fiber-based sensor devices. Fibers can be etched or polished so that the deposited material can be very close (a few microns) to the core, thus interacting with the guided field producing feedback and evanescent wave coupling.

Microscopic structures of chromium were deposited on the outer surface of etched fibers by 500-fs, 248-nm pulses. Pulse energy density was again in the range below 100 mJ/cm^2. The chromium targets were 250–800-Å-thick thin films formed on fused silica substrate as above. The structure was deposited in a point-to-point manner by accurate alignment of the fiber axis along the motion axis.

Figures 7(a) and 7(b) depict closeup views of a chirped gratinglike structure comprising submicrometer features as deposited on the flat surface of Andrew D-type fiber with a 125-μm outer diameter. In Fig. 7(c) an example appears of a periodic structure developed on an etched fiber having an outer diameter of ~35 μm. The size of the spots deposited in this case is ~2 μm. The structure is used in the ongoing investigation of guided wave coupling effects. It is clear that for single-mode fibers more complex asymmetric etching procedures must be applied to approach the well-confined field in the fiber core.

The results above, however, demonstrate the unique potential of the method for fabricating microstructures onto nonplanar and high-curvature surfaces. Such operations would be proved significant in the further development of optical-fiber sensors and optical telecommunications devices, including alternative Bragg fiber gratings, rocking filters, fiber polarizes, and evanescent-wave fiber sensors.

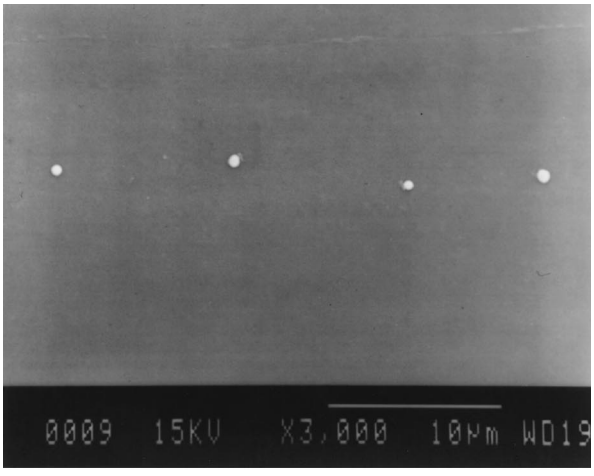

(a)

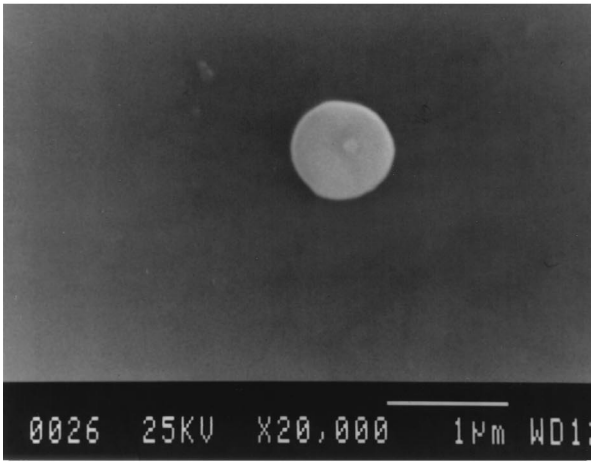

(b)

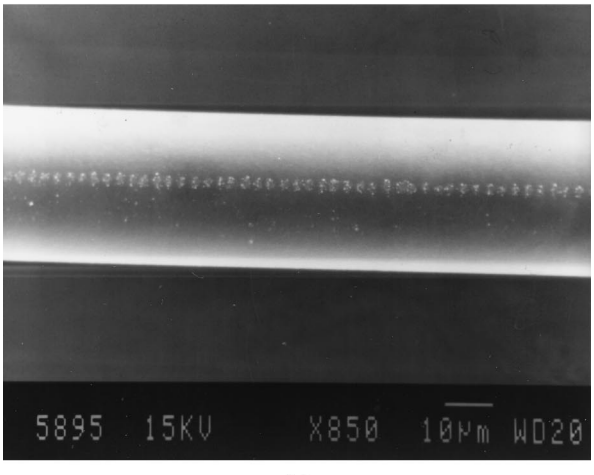

(c)

Fig. 7. (a), (b) Closeup views of gratinglike structure developed on D-type optical fiber revealing submicrometer features and (c) 2-μm features periodically deposited on a 35-μm-diameter optical fiber.

4. Conclusions

The use of ultrashort excimer-laser radiation has proved advantageous in the direct development of computer-generated holograms and other diffractive optical microstructures. Ultrashort laser pulses produce a better etching quality, thus improving the already established method of excimer-laser microetching. The reduced thermal effects provide a high spatial resolution and a relatively large etching aspect ratio. Furthermore the potential of microprinting metals and oxide structures onto optical surfaces has been demonstrated by the fabrication of metal diffractive structures onto planar and nonplanar surfaces. The growth of InO_x diffractive structures represents a further advance verifying the potential for the development of active microstructures. In addition, the unique scheme for direct fabrication of microstructures onto nonplanar surfaces has been demonstrated by the production of submicrometer features onto etched optical-fiber surfaces.

The complementary etching and printing methods presented rely on purely physical noncontact pro-

cesses requiring no additional processing procedures. They represent single-step alternative microfabrication approaches, alleviating the limitations of well-established lithographic methods. Their high versatility and unique potential may lead to novel developments. Further effort is currently being put on the growth of optically active microstructures.

Research supported by the European Union through the Large Installations Plan, "Ultraviolet Laser Facility," at the Foundation for Research and Technology-Hellas, under European Union contract ERBFMGECT950021 and the Hellenic Ministry of Development, in the framework of the national project National Optoelectronic Vision Systems as well as Regional Development Program and Human Resources support projects. Two CGH designs were kindly supplied by Trevor J. Hall.

References

1. J. W. Goodman, ed., *International Trends in Optics* (Academic, London, 1991).
2. G. J. Swanson and W. B. Veldkamp, "Diffractive optical elements for use in infrared systems," Opt. Eng. **28,** 605–608 (1989).
3. T. Yatagai, H. C. Bolstad, H. Hashizume, S. Kobayashi, and M. Seki, "Optimization of gradient-index computer-generated hologram," in *Computer and Optically Formed Holographic Optics*, I. Cindrich and S. H. Lee, eds., Proc. SPIE **1211,** 191–195 (1990).
4. E. Pawlowski and B. Kuhlow, "Antireflection-coated diffractive optical elements fabricated by thin-film deposition," Opt. Eng. **33,** 3537–3546 (1994).
5. L. Ristic, ed., *Sensor Technology and Devices* (Artech House, Boston, 1994).
6. N. A. Vainos, S. Mailis, S. Pissadakis, L. Boutsikaris, P. Parmitter, P. Dainty, and T. J. Hall, "Excimer laser use for microetching computer-generated holographic structures," Appl. Opt. **35,** 6304–6319 (1996).
7. G. P. Behrmann and M. T. Duignan, "Excimer laser micromachining for rapid fabrication of diffractive optical elements," Appl. Opt. **36,** 4666–4674 (1997).
8. J. Bohandy, B. F. Kim, and F. J. Adrian, "Metal deposition from a supported metal film using an excimer laser," J. Appl. Phys. **60,** 1538–1539 (1986).
9. J. Bohandy, B. F. Kim, F. J. Adrian, and A. N. Jette, "Metal deposition at 532 nm using a laser transfer technique," J. Appl. Phys. **63,** 1158–1162 (1988).
10. E. Fogarassy, C. Fuchs, S. de Unamuno, F. Kerherve, and J. Perriere, "High *Tc* superconducting thin film deposition by laser induced forward transfer," Mater. Manuf. Processes **7,** 31–51 (1992).
11. E. Fogarassy, C. Fuchs, F. Kerherve, G. Hauchecorne, and J. Perriere, "Laser-induced forward transfer of high-T_c YBaCuO and BiSrCaCuO superconducting thin films," J. Appl. Phys. **66,** 457–459 (1989).
12. E. Matthias, M. Reichling, J. Siegel, O. W. Kading, S. Petzoldt, H. Skurk, P. Bizenberger, and E. Neske, "The influence of thermal diffusion on laser ablation of metal films," Appl. Phys. A **58,** 129–136 (1994).
13. T. D. Bennett, C. Grigoropoulos, and D. J. Krajnovich, "Near-threshold laser sputtering of gold," J. Appl. Phys. **77,** 849–864 (1995).
14. J. Ihlemann and B. Wolff-Rottke, "Excimer laser micromachining of inorganic dielectrics," Appl. Surf. Sci. **106,** 282–286 (1996).
15. P. P. Pronko, S. K. Dutta, D. Du, and R. K. Singh, "Thermophysical effects in laser processing of materials with picosecond and femtosecond pulses," J. Appl. Phys. **78,** 6233–6240 (1995).
16. S. Preuss, E. Matthias, and M. Stuke, "Subpicosecond UV-laser ablation of Ni films," Appl. Phys. A **59,** 79–82 (1994).
17. T. Götz and M. Stuke, "Short-pulse UV laser ablation of solid and liquid metals: indium," Appl. Phys. A **64,** 539–543 (1997).
18. X. Liu, D. Du, and G. Mourou, "Laser ablation and micromachining with ultrashort laser pulses," IEEE J. Quantum Electron. **33,** 1706–1716 (1997).
19. P. Simon and J. Ilhemann, "Machining of submicron structures on metals and semiconductors by ultrashort UV-laser pulses," Appl. Phys. A **63,** 505–508 (1996).
20. I. Zergioti, S. Mailis, N. A. Vainos, P. Papakonstantinou, C. Kalpouzos, C. P. Grigoropoulos, and C. Fotakis, "Microdeposition of metal and oxide structures using ultrashort laser pulses," Appl. Phys. A **66,** 579–582 (1998).
21. C. Grivas, D. S. Gill, S. Mailis, L. Boutsikaris, and N. A. Vainos, "Indium oxide thin-film holographic recorders grown via excimer laser reactive sputtering," Appl. Phys. A **66,** 201–204 (1998).